lubricants

MDPI

Article

Evaluating the Tribological Behaviour in Cutting Operations Using a Modified Ball-on-Disc Open Tribotester

Belal G Nassef [1,2,*], Florian Pape [1], Gerhard Poll [1], Jan Schenzel [3], Benjamin Bergmann [3] and Berend Denkena [3]

[1] Institute of Machine Design and Tribology, Leibniz University of Hanover, 30823 Hannover, Germany; pape@imkt.uni-hannover.de (F.P.); poll@imkt.uni-hannover.de (G.P.)
[2] Production Engineering Department, Faculty of Engineering, Alexandria University, Alexandria 21544, Egypt
[3] Institute for Production Engineering and Machine Tools, Leibniz University of Hanover, 30823 Hannover, Germany; schenzel@ifw.uni-hannover.de (J.S.); bergmann@ifw.uni-hannover.de (B.B.); denkena@ifw.uni-hannover.de (B.D.)
* Correspondence: nassef@imkt.uni-hannover.de

Abstract: Predicting the tribological behaviour in the secondary shear zone in the metal-cutting processes is considered a significant challenge in contemporary research. This work investigated the frictional performance in the secondary shear zone of a planing process using a modified ball-on-disc open tribometer. The values of the coefficient of friction (COF) were tracked between an AISI4140 + QT disc (chip) and a cemented carbide ball (cutting tool) coated with TiAlN under three contact pressures of 0.5, 1, and 2 GPa at a range of sliding speeds starting from 0.2 m/s to 1.6 m/s. The tests were conducted under both dry and lubricated conditions using three commercial cutting fluids of CSF 35 straight oil, Vasco 6000, and Zubora 67H emulsions. Also, the MWFs were tested for their rheological properties and wettability. The tribometer results validated the same COF trend as that in the actual metal-cutting experiments, particularly at 0.5 and 1 GPa in dry conditions. Moreover, Zubora 67H emulsion is proven to be the optimal choice due to it reducing the COF between the rubbing contacts by up to 78%. Furthermore, it showed the lowest contact angle and viscosity index, revealing its ability to easily penetrate, especially at higher temperatures, within the secondary cutting zone.

Keywords: open tribometer; ball-on-disc; rheology; wettability; metal cutting fluid; tribology; planing process

Citation: Nassef, B.G.; Pape, F.; Poll, G.; Schenzel, J.; Bergmann, B.; Denkena, B. Evaluating the Tribological Behaviour in Cutting Operations Using a Modified Ball-on-Disc Open Tribotester. *Lubricants* **2024**, *12*, 77. https://doi.org/10.3390/lubricants12030077

Received: 18 January 2024
Revised: 19 February 2024
Accepted: 27 February 2024
Published: 28 February 2024

1. Introduction

Metal-working fluids (MWFs) have been in use since the 19th century, participating in the total production cost by up to 17% [1,2]. Until now, conventional mineral oil has been considered the most common cutting fluid that is widely used in machinery in either straight form or emulsified with water. Also, petroleum products, which exist in mineral oils, were found to have a notable share in up to 85% of the overall consumed MWFs [1,3]. The main reasons behind that are attributed to the mineral oil's outstanding lubricating characteristics as well as the significant impact of the additives and modifiers used to improve its tribological, cooling, and physicochemical properties [4–6].

Despite using the MWFs to reduce heat and improve tribological performance, there is still a great need of improving the machinability of materials through optimising the cutting process parameters [7]. These parameters, particularly in terms of cutting speeds and feed rates, have become a focal point in contemporary manufacturing. By optimising these parameters, elevated cutting regimes can be achieved, ultimately boosting productivity in cutting operations [8]. Consequently, this increase in productivity is accompanied by a significant rise in temperatures due to high frictional forces in the cutting interfaces, which, in turn, accelerates tool wear and leads to rapid deterioration of the cutting tools.

To address this challenge, the previous literature has put forth two primary solutions. The first solution involves the development of a precise and reliable model for predicting temperature and tribological parameters under various cutting parameters, utilising finite element analysis [9]. However, because of the substantial variation in relative speeds between the primary and secondary zones and the difficulty in maintaining constant pressure across the cutting interfaces [10], this approach can yield only approximate values without considering other cutting parameters. As a result, this solution falls within the realm of providing approximate validation for experimental data, rather than being the primary source of reliance.

Turning to the second one, this consists of employing the experimental investigation to track the tribological and thermal parameters along the cutting operation. It involves using either actual cutting operations or customised tribotesters [11]. Regarding the actual cutting, conventional sensors, such as dynamometers, have been employed to track the normal and tangential forces during the cutting action in order to obtain the resultant force, which is used in friction coefficient (COF) calculations. Also, the temperature is recorded along the cutting process. However, it is still difficult to comprehensively explain the temperature variations and local contact pressures along the cutting interfaces, especially in the secondary zone [12].

Therefore, customised tribotesters, such as ball-on-disc [13] and pin-on-ring [14], emerged as efficient solutions to precisely control the contact conditions. They are mainly based on initiating a relative motion between the ball or the pin, which is fabricated from the cutting tool material and the disc or the ring, which is made of the same workpiece material. In prior research, Liu and Pape explored the suitability of the EHL ball-on-disc test rig, pin-on-ring, and pin-on-plate tribotesters for investigating metalworking fluids (MWF). Their studies revealed insights into the impact of boundary films on the frictional properties during metal cutting [15,16]. A previous research article considered employing a cylinder-on-disc tribometer in order to evaluate frictional forces and wear values for different coated cylinders at long distances and a high sliding speed range of 0.5–3 m/s. It was found that applying Al2O3 in coating has a negative effect on wear characteristics, especially at lower speeds. Conversely, TiN and TiC coatings showed outstanding wear resistance throughout the overall speed range. However, the tests were kept running on the same contact surface without regeneration with a limited contact pressure value of less than 10 MPa [17].

Another research work conducted by Olsson et al. [18] studied the relation between the sliding wear and sliding speed of a cemented carbide cutting tool coated with TiC and another of high-speed steel coated with TiN. They employed a modified pin-on-ring setup for the test with a refreshed surface. It was found that the critical cutting speeds for TiC pins were between 150 and 200 m/min, while the TIiN pins accounted for 50 to 75 m/min. The wear behaviour after those speeds started to increase exponentially, showing higher values in the case of TiN-coated pins due to thermal softening. Moreover, they compared the wear mechanisms with that in the actual cutting from previous literature, revealing nearly the same mechanisms. While their published article marked a significant achievement, it is worth noting that the sliding distance range was restricted, and the pressure values were still insufficient (15 MPa).

Despite substantial efforts in using tribotesters to simulate real cutting processes, the techniques employed have fallen short of delivering satisfactory results. This is primarily due to two main reasons. First, most of these methods often work on the same surface without ongoing contact regeneration (closed tribometers), which does not align with machining requirements. In machining, the cut surface continually interacts with the tool, either the flank or rake surfaces, only once before the chip forms and is subsequently removed [7,8]. The second concern relates to the constrained sliding distance, pressure, and velocity ranges, which must be broadened to encompass the full spectrum of actual cutting conditions.

Several research articles proposed modified open tribotesters as an efficient solution for the previous issues [19,20]. Rech et al. [21] developed an open tribometer based on the

pin-on-ring setup attached to a CNC lathe to mimic the cutting process through studying a wide range of contact pressures (up to 3 GPa) and sliding speeds (up to 5 m/s). Their aim was to study the frictional behaviour along with the heat partition parameter. They found that the heat parameter and COF kept a drastic decrease while the cutting velocity increased on dry conditions. However, in lubricated cases, those curves were reaching near constant values, even at higher cutting velocities. The previous results were confirmed by the ABAQUS simulation tool in the same study with a maximum difference of 20%.

A recent investigation developed a high-speed pin-on-bar tribometer in order to evaluate the COF in the drilling of C45 steel. The study involved evaluating and comparing the COF when utilising the test rig as both a closed and open system. It was revealed that the COF in the closed system was higher compared to the open system. The main reason behind that was attributed to the increased contact area in the closed system, resulting in elevated temperatures and the promotion of plastic deformation. Additionally, there was a clear direct correlation between the COF and the applied contact pressure in the open system, while it displayed an inverse relationship with sliding velocities. In the closed system, the COF exhibited an inverse relationship with both contact pressure and sliding velocities [22].

Based on the previous literature, it can be observed that most of the tribotesters are based on using a pin to simulate the cutting tool. However, there is a significant shortage in the articles concerned with employing a ball-on-disc configuration in evaluating COF for cutting operations. A ball-on-disc tribotester is the most common device used in evaluating the tribological characteristics of lubricants and surface interactions [23,24] due to its wider speed range, high stability, and affordability [25]. Previous research articles have considered the application of ball-on-disc with a contra-rotation idea to evaluate the scuffing phenomenon. The main advantage behind this was the higher operating speeds that can be reached, with negligible entrainment velocity, which prevents the elastohydrodynamic film formation maintaining the boundary condition. Also, this technique allows for more uniform distributed along the disc surface with nearly constant contact pressure [26,27].

Hence, the objective of this study was to examine the influence of both dry and lubricated conditions on a specially designed open ball-on-disc tribometer that incorporates contra-rotation, simulating the secondary zone in the cutting process. The investigation involves the use of three different types of MWFs to evaluate their impact on frictional behaviour. The obtained results are to be compared with those derived from the real cutting process using a planning operation. Additionally, the physical characterisation of cutting fluids, employing viscosity measurements, and wettability analysis were incorporated to illustrate the behaviour of each cutting fluid.

2. Materials and Methods

2.1. Materials and Characterisation

In this study, AISI4140 + QT steel was selected as the disc material. This choice was influenced by its extensive use in highly stressed components, such as crankshafts in critical industrial applications. This type of steel possesses outstanding mechanical properties in terms of high strength ($\geq$1000 MPa) and toughness [28]. As for the balls, they were produced from tungsten carbide with 6% cobalt (Co). Notably, the average surface roughness values (Ra) were adjusted to be Ra = 0.07 µm for the steel disc, while the ball's surface retained a value of Ra = 0.02 µm. Additionally, the experimental setup included the application of three distinct commercial MWFs to the rubbing contact, which were Vascomill CSF 35 oil and BLASER Vasco 6000 emulsion, both from the Blaser Swisslube company, Switzerland, and the Zubora 67H emulsion from Zeller + Gmelin GmbH, Eislingen, Germany. Table 1 shows detailed information about the applied MWFs.

Table 1. Properties of the proposed base oils.

Item	Vascomill CSF 35 Oil	Blaser Vasco 6000	Zeller + Gmelin Zubora 67H Extra
Viscosity at 40 °C	35 mm^2/s	42 mm^2/s	39 mm^2/s
Density at 20 °C	0.90 g/cm^3	0.99 g/cm^3	0.98 g/cm^3
Structure	Ester-based oil	Fully synthetic emulsion based on 10% ester-oil and 90% deionized water	Semi-synthetic emulsion based on 10% mineral-oil and 90% deionized water
Flash point °C	310	129	>100

2.2. FTIR Anaylsis

The chemical composition of MWFs was evaluated by analysing the functional groups present in their structure using Fourier transform infrared spectroscopy (FTIR). A Perkin Elmer Spectrum 100® FTIR (Perkin Elmer Company, Hamburg, Germany) was utilised for this purpose. The analysis covered a broad spectrum of wavenumbers, ranging from 650 to 4500 cm^{-1} with a resolution of 0.5 cm^{-1}. The acquired spectra were then compared with the manufacturer specifications for each cutting fluid to facilitate a comprehensive discussion.

2.3. Rheological Behavior

The physical characteristics of the applied MWFs were assessed in terms of their rheological behaviour using a rotational rheometer (Kinexus Prime lab + Netzsch GmbH, Germany), as illustrated in Figure 1. A sample volume of 0.3 mL of the base oil was introduced into the testing setup to be tested over a wide spectrum of shear rates, starting from 0.1/s to 100/s. Tests were carried out at various temperatures starting from 20 °C to 100 °C to analyse the temperature-dependent behaviour of each cutting fluid with two repetitions.

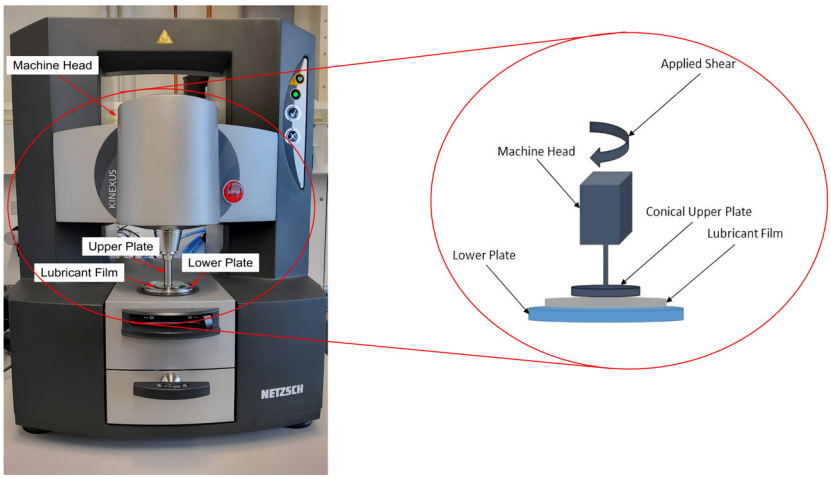

Figure 1. Experimental arrangement for rheometer testing.

2.4. Ball-on-Disc Open Tribometer

The experimental setup used in this study is based on an optical ball on disc tribometer used to measure the lubricant film thickness in the elastohydrodynamic lubrication condition (EHL). The setup originally depends on a pure rolling action between a rotating glass disc and a free ball loaded with a lever mechanism. However, the tribotester was developed in this study by replacing the glass disc with an AISI4140 + QT steel one, which was of the same workpiece (chip) material. Regarding the ball, it was manufactured from cemented carbide (WC-6Co) coated with TiAlN, simulating the cutting tool material. A specific shaft was designed to connect the ball to a driving motor in order to achieve the contra-rotation action. A Burster torque sensor of 2 N·m range and 0.2 N·m sensitivity,

which was operated using the power source, was placed between the ball shaft and the motor to evaluate the torque consumed in the contra-rotation action, as shown in Figure 2.

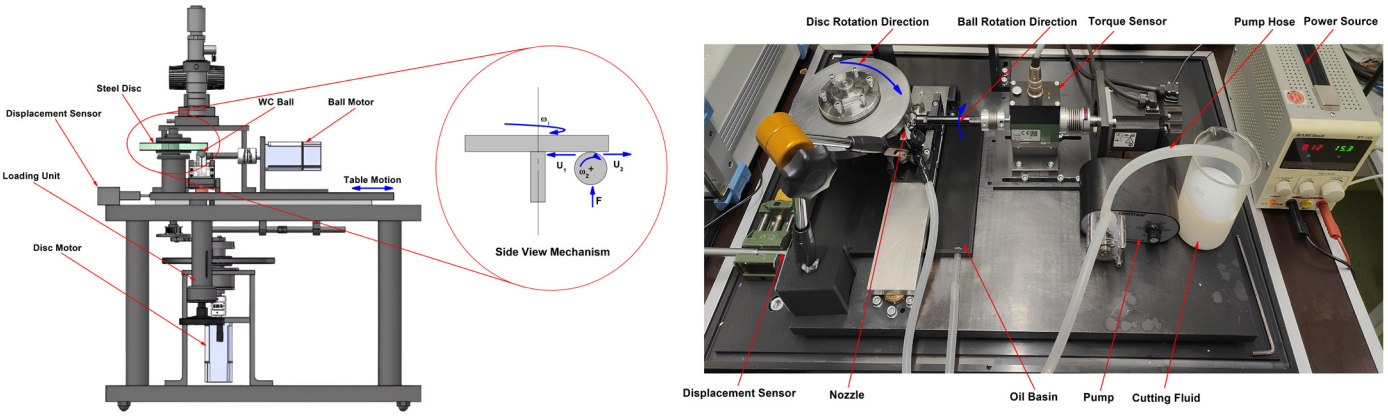

Figure 2. Open ball-on-disc tribotester: (**a**) mechanical drawing and (**b**) actual test setup.

The test started with loading the ceramic ball against the rotating disc to reach three different contact pressures of 0.5, 1, and 2 GPa. Then, the ball began to rotate with ω2 in the opposite direction of the disc (ω1), but with the same sliding speed to achieve the contra-rotation action with zero entrainment speed. For each loading condition, four sliding speeds of 0.1, 0.2, 0.4, and 0.8 m/s were tested, separately, at each loading condition to record the frictional behaviour at different positions on the secondary cutting shear zone. For each sliding speed, a fresh surface was exposed to testing in order to maintain an open system. This was achieved by moving the table holding the disc with 150 µm distance before switching to the subsequent sliding speed, which was controlled by a displacement sensor of sensitivity of 100 µm, as shown in Figure 2. The testing speeds were to be multiplied by 2 due to the contra-rotation action (according to Equation (1)) to cover a speed range of 0.2 m/s to 1.6 m/s:

$$Us = U1 - U2, \quad (1)$$

where U1 is the sliding velocity of the disc and U2 is the sliding velocity of the ball.

Firstly, the test was conducted at the dry condition to obtain a standard COF value for comparison, and then the COF was evaluated under lubricated conditions using the three types of MWFs at each contact pressure and sliding speed. A Grothen DC 12V pump was employed to supply each fluid to the contact zone. After this, the frictional torque values with time were recorded using a specially designed LabVIEW program, and then the COF was calculated according to Equation (2). Each test was repeated two times to ensure the reliability of results with an error of up to ±0.3%.

$$\mu = Tf/Fr, \quad (2)$$

where Tf is the average frictional torque value, F is the applied normal load, µ is the average COF value, and r is the ball radius.

2.5. Wettability Analysis

The wettability characteristics of the MWFs were evaluated by measuring the contact angle of each fluid with the steel surface. A Krüss EasyDrop (FM40, KRÜSS GmbH, Hamburg-Nord, Germany) goniometer device was employed for this type of testing by placing a 0.3 µL liquid droplet to the steel substrate at room temperature (20 °C). Subsequently, the interfacial contact between the steel substrate and the droplet was captured

by a high-quality CCD camera, and the contact angle was evaluated using SW21 (DSA 1) software with four repetitions.

2.6. Orthogonal Cutting

For orthogonal cutting tests, a planing test rig was used. Due to the linear direct drive, this test rig enabled a cutting speed of up to V_c = 500 m/min and maximum forces of Fmax = 7.2 kN. A Kistler Dynamometer of type 9257B was used to measure the process forces. A high-speed camera of the type Photron Nova S20 was used at a frame rate of 15,000 FPS and an exposure of 1/50,000 s. Due to the image resolution of 1024 × 1024 px and the 14× magnification, the minimal length, which can be measured, was 1.42 µm. The experimental setup can be seen in Figure 3. Quenched and tempered steel AISI4140 + QT was used as the workpiece material. As shown in Figure 3c, the workpiece had a section with increasing height with 2.5 µm/mm of length 100 mm and a section of constant height with a length of 20 mm. Therefore, in every experiment, the uncut chip thickness varied from h = 0 µm up to h_{max} = 0.1 mm. The minimal chip thickness h_{min} was determined using the high-speed recordings in order to calculate the mechanical load on the flank face. For all experiments, a chip width of b = 2 mm was used. As a tool, cemented carbide of the type K68 from Kennametal with an additional TiAlN-coating with a thickness of 3 µm and a geometry of the type SNMA 120408 was used. Due to the tool holder, the rake angle was set to $\gamma = 0°$; therefore, a clearance angle of $\alpha = 15°$ was ground on the tool. Additionally, the cutting tool had a symmetric cutting edge rounding of $\overline{S}$ = 37 µm. Every cutting experiment was repeated twice. A detailed description of the measurement errors of the method for determining the normal and tangential stress at the cutting edge can be found in [29]. The measurement uncertainty for the normal stress at the rake face was 6.3%. Due to the short cutting time of 0.06 s, geometric changes to the cutting wedge caused by a wear-like crater or flank wear were negligible.

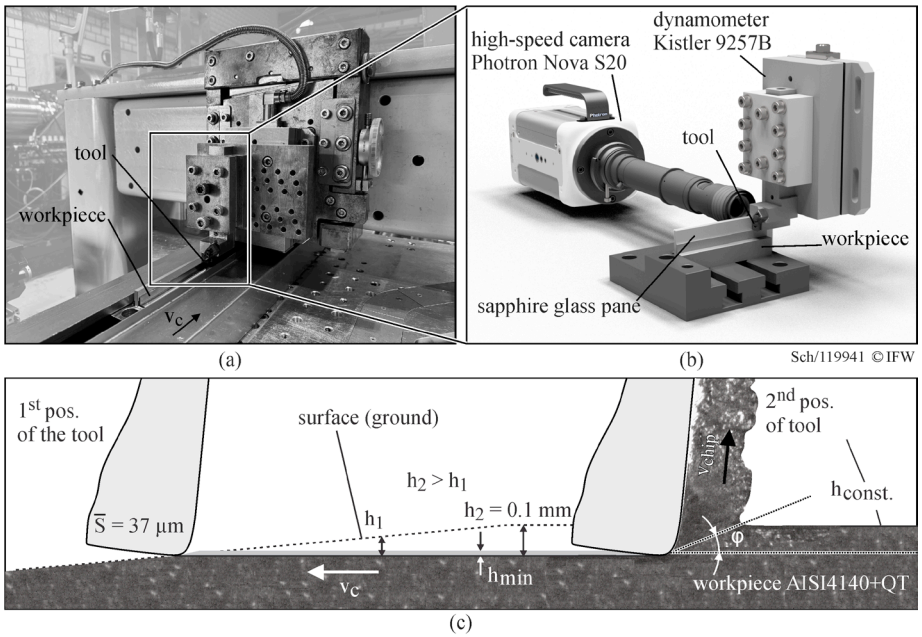

Figure 3. (**a**) Planing test rig and (**b**) experimental setup for high-speed recordings of chip formation. (**c**) Preparation for the workpiece according to Bergmann [29].

3. Results and Discussion

3.1. FTIR Results

The FTIR spectral analysis of cutting fluids, including CSF 35, Vasco 6000, and Zubora 67H, revealed distinctive features, as shown in Figure 4. CSF 35 exhibited a notable absence of O-H bending, unlike Vasco 6000 and Zubora 67H, where a pronounced

O-H group was observed at 3362 cm^{-1}, indicating higher water content. Additionally, CSF 35 displayed C-H bending at 2922, 2852, 1463, 1380, and 724 cm^{-1}, along with a strong carbonyl group (C=O) at 1745 cm^{-1} and C-O functional groups at 1163 and 953 cm^{-1}. The CSF 35 FTIR spectrum confirmed its ester-based nature, as shown in Figure 4a.

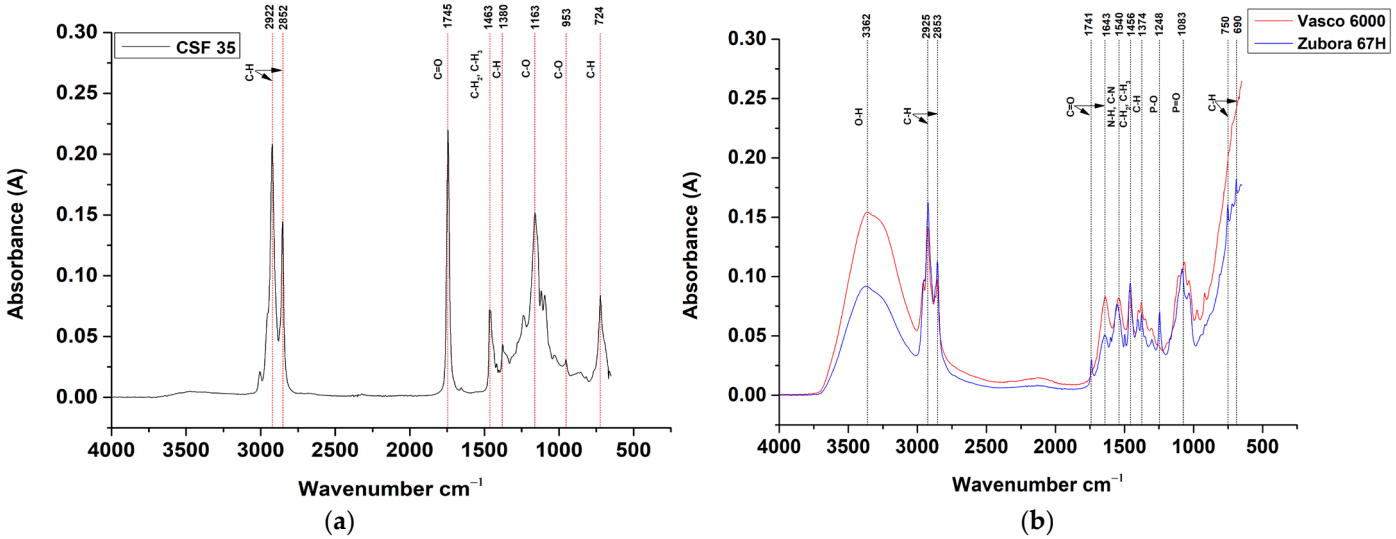

Figure 4. FTIR spectra for (**a**) CSF 35 oil; (**b**) Vasco 6000 and Zubora 67H emulsions.

In contrast, Vasco 6000 and Zubora 67H spectra demonstrated differences, as depicted in Figure 4b. Both exhibited a wide O-H group at 3362 cm^{-1}, with Vasco 6000 displaying a stronger peak, suggesting variations in water content. Similar C-H stretching bands were observed with lower intensities, accompanied by an additional peak at 690 cm^{-1}. Notably, Zubora 67H showed a barely observable carbonyl group at 1741 cm^{-1}, while Vasco 6000 presented a significant carbonyl peak at 1643 cm^{-1}. The appearance of the amide group II, indicated by N-H bending and C-N stretching vibrations at 1540 cm^{-1}, suggested the incorporation of amide compounds in the base-oil, such as alkanolamines. Peaks at 1248 and 1083 cm^{-1} were attributed to phosphoric acid ester, aligning with manufacturer specifications.

3.2. Rheological Behavior

Figure 5 illustrates the viscosity–shear rate profiles of the applied MWFs across a wide range of operational temperatures, including various shear rates. Initially, all cutting fluids exhibited a Newtonian behaviour at temperatures of up to 40 °C. However, a transition to non-Newtonian behaviour became evident, particularly in the emulsion-based oils, as the temperature surpassed 40 °C, leading to an obvious shear thinning trend at 60 °C. This shear-thinning characteristic became more pronounced at 80 °C and persisted up to 100 °C. Notably, CSF 35 exhibited a remarkable thermal stability by maintaining its viscosity nearly constant without significant changes across this temperature range.

Regarding shear thinning behaviour, it can mainly be considered a combination of two main reasons. The first one involves the re-orientation of the hydrocarbon chains in the emulsions, which reduces the viscosity value while the shear rate increases [30]. This phenomenon is linked to the dynamic rearrangement of molecular structures within the emulsion, facilitating a more streamlined flow pattern. The other one is attributed to the alignment of additives embedded in the emulsion's structural matrix. This alignment occurs along the direction of shearing flow, preventing collisions between particles and contributing significantly to the observed shear-thinning phenomenon [31–33]. Despite the limited literature, a previous study examined the shear-thinning behaviour of a drilling paraffin-based suspension. The primary objective was to predict the gravitational separa-

tion of solid particles within the cutting fluid. The study validated that the paraffin-based suspension exhibited the anticipated shear-thinning behaviour [34].

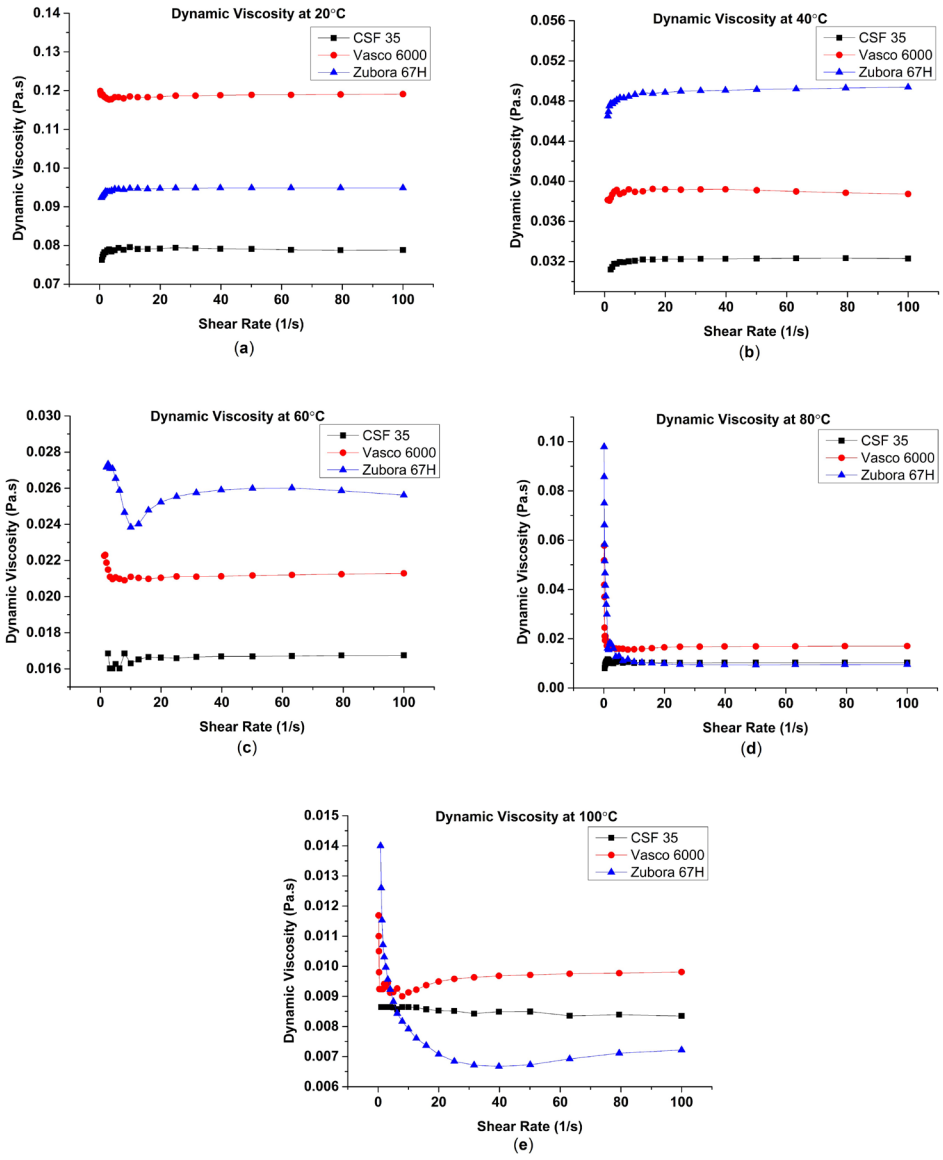

Figure 5. Dynamic viscosity behaviour at different shear rates for each cutting fluid at (**a**) 20 °C, (**b**) 40 °C, (**c**) 60 °C, (**d**) 80 °C, and (**e**) 100 °C.

Figure 6a depicts the temperature-dependent characteristics of each cutting fluid over a broad temperature range. Notably, the dynamic viscosity values exhibited a substantial reduction upon reaching 40 °C. Subsequently, the viscosity trend demonstrated a gradual decrease until reaching 100 °C. A prominent observation is the apparent variation in viscosity patterns, with Vasco 6000 displaying the highest viscosity and CSF 35 registering the lowest. Based on this observation, a conclusion can be drawn regarding the efficacy of emulsifiers and surfactants employed in emulsion-based oils, such as phosphoric acid ester, which was confirmed by FTIR results. These additives play a crucial role in stabilising the small droplets, preventing their easy separation or coalescence, distinguishing them from the properties exhibited by CSF 35 oil [35,36]. The observed decline in viscosity at elevated temperatures is principally ascribed to the weakening impact on molecular bonds inherent within the oil structure due to the increased thermal energy. This leads to increasing the fluidity and reducing shear resistance of the fluid [37,38].

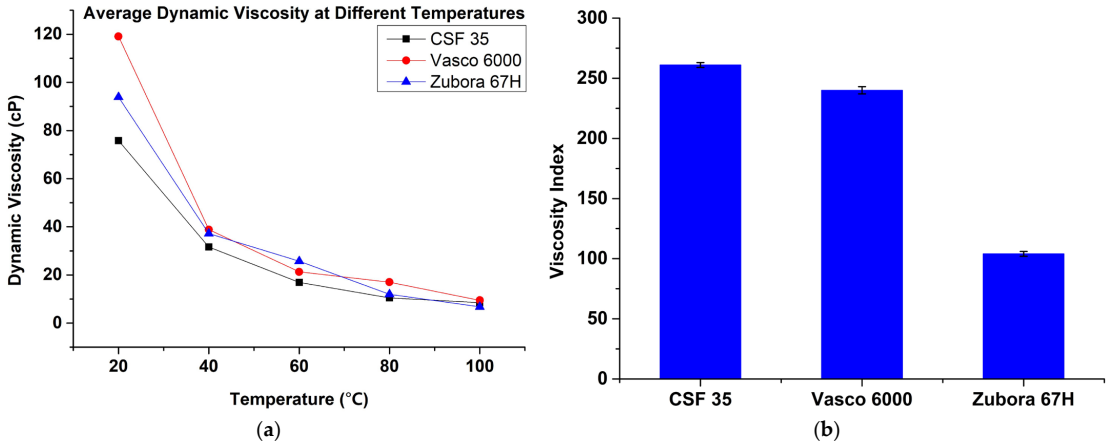

Figure 6. (**a**) Temperature-dependent viscosity behaviour and (**b**) viscosity index values for the cutting fluids.

Regarding Figure 6b, it displays the viscosity index of the applied cutting fluids, revealing the highest value for CSF 35. Subsequently, Vasco 6000 was observed, followed by Zubora 67H, highlighting the ability of CSF 35 to hold its rheological behaviour over a wide range of temperatures. Conversely, Zubora 67H, being a semi-synthetic emulsion, cannot maintain its viscosity at higher temperatures. This distinct behaviour underscores the effectiveness of Zubora 67H in facilitating easier chip removal, aligning with discussions from prior investigations [39].

3.3. Frictional Characteristics

Figure 7 depicts the average coefficient of friction in dry conditions across three applied pressures at varying sliding speeds. The results indicate a consistent rise in frictional behaviour with increasing sliding speed under loading conditions up to 1 GPa, resulting in a COF increase of up to 85%. However, a contrasting trend emerged when the loading condition surpassed 1 GPa, showing a notable reduction of nearly 20% in the COF value. Moreover, it is noteworthy that the observed COF range aligned closely with that encountered in actual metal cutting operations, particularly at the point of maximum contact pressure, falling within the range of 0.40 to 0.49. This relation highlights the practical relevance and applicability of the study's findings to real-world metal cutting scenarios, which is to be shown in the next subsections.

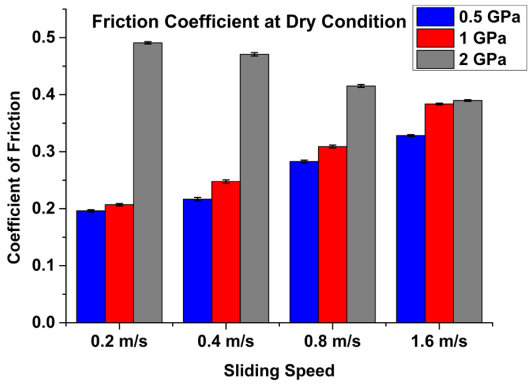

Figure 7. Friction coefficients under varying speeds and loading conditions in a dry environment.

The observed trend of the decreasing coefficient of friction (COF) at 2 GPa finds support in the existing literature, offering valuable insights into this phenomenon. Rech et al. [40] anticipated this trend, and experimental confirmation was subsequently provided by Zemzemi et al. [8]. The latter researchers attributed this behaviour to the heightened

dissipation of frictional heat at elevated sliding speeds (up to 4 m/s), particularly in the secondary shear zone under a contact pressure of 2.5 GPa. This suggests that as sliding speeds increased, there was a corresponding increase in the dissipation of heat generated by friction, contributing to the reduction in COF.

In another investigation, the adoption of identical workpiece and cutting tool materials, albeit with a different open tribotester, yielded analogous findings. The study reported a consistent trend, noting a decrease in the coefficient of friction (COF) during tests conducted at higher pressures, spanning from 2 GPa to 3.5 GPa. The observed behaviour persisted with increasing sliding speeds across a range from 0.1 m/s to 4 m/s. The researchers attributed this phenomenon to the minimal impact of surface irregularities or micro-features on the friction coefficient, particularly at elevated sliding velocities, reaching up to 1.5 m/s. These irregularities appeared to be less influential under high-speed conditions, likely due to being carried away by the rapid motion [7].

Furthermore, Lakner et al. [28] shifted their focus to the influence of plastic deformation and subsequent thermal softening as key factors in diminishing the coefficient of friction (COF). The research conducted a thorough comparative analysis of frictional behaviour, examining two distinct workpiece materials, Ti-6Al-4V and 42CrMo4 + QT, in conjunction with a cemented carbide tool coated with TiCN. Under conditions of higher pressures (of up to 1.5 GPa) and sliding speeds, the study suggested that plastic deformation at the contact interface could induce thermal softening. This transformative process renders the material more pliable, resulting in a remarkable reduction in frictional resistance and, consequently, contributing to the observed decline in COF.

Figure 8 illustrates the frictional characteristics of each cutting fluid under various normal pressures and sliding velocities, in comparison to the dry condition. At the lowest pressure of 0.5 GPa, the frictional trend consistently increased for all lubrication conditions, aligning with the behaviour observed in the dry case. Nevertheless, a noteworthy decrease in the friction coefficient was observed in the lubricated condition, ranging from 11% to 64%, as compared to the dry case. Emulsion-based fluids exhibited the most significant reduction, with Vasco 6000 showing a decrease of up to 45%, and Zubora 67H recording a substantial reduction of 64%.

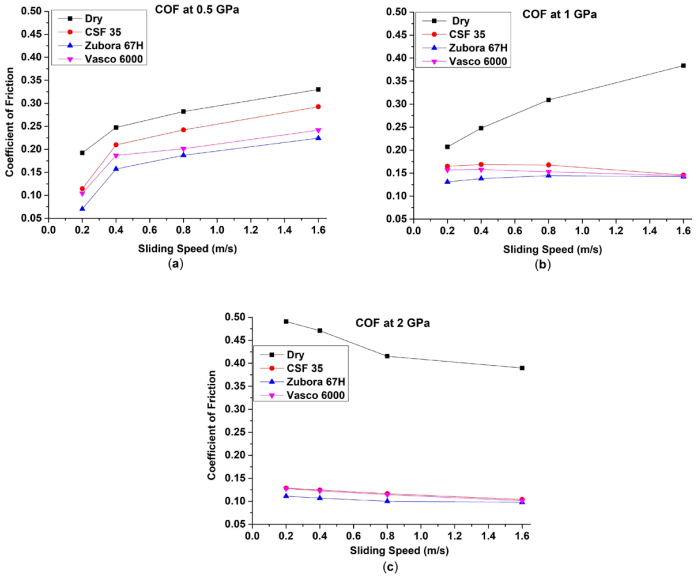

Figure 8. Average friction coefficient values at various sliding speeds under normal pressures of (**a**) 0.5 GPa, (**b**) 1 GPa, and (**c**) 2 GPa.

Turning to 1 GPa, it was observed that the frictional trend showed a slight change in the values when increasing sliding velocities, except for the values recorded at the highest speed of 1.6 m/s, as shown in Figure 8b. However, the cutting fluids kept the

same behaviour as the emulsion-based fluids, especially Zubora 67H, which showed better performance compared to CSF 35 oil. In this case, the highest reduction percentage accounted for up to 63%. Next came the uppermost contact pressure (Figure 8c), showing a more stable trend across the sliding speed range for all cutting fluids. The maximum reduction was fulfilled at this case by reaching up to 78% for Zubora 67H.

The primary mechanism driving the reduction in coefficients of friction (COF) is attributed to the formation of a physical barrier facilitated by the presence of longer hydrocarbon chains in ester-based fluids. These longer chains, enriched with prominent C-H groups, created a robust protective layer, thereby reducing friction. Additionally, the polar nature of carbonyl groups enhanced adsorption of the hydrocarbon chains onto the metal surface, contributing to the overall friction reduction [41–43]. In the case of emulsion-based oils, the friction-modifying effect is associated with the presence of polar additives, such as hydroxyl stretching band (O-H) and N-H, as well as C-N amide groups introduced through alkanolamides. Moreover, the FTIR spectrum revealed the presence of phosphorous-based additives, consistent with the manufacturer specifications, with no indications of sulphur or chlorine. This confirms that the EP (extreme pressure) additives in the emulsions were phosphorous based. Notably, Zubora 67H displayed a significant presence of phosphorous-based additives. These EP additives are significantly activated at extreme conditions, such as higher loading conditions and speeds, leading to a chemical reaction with the metallic surface and the forming of a robust thicker boundary film. This boundary film may contain iron phosphate, iron oxide, and organic phosphine [44].

This observation was validated by Ma et al. [45] through a comparative analysis of two cutting fluids during the drilling process of Ti-6Al-4V. Their study revealed that the utilisation of the cutting fluid with elevated levels of EP additives under increased drilling conditions resulted in the formation of irregularly dispersed and thicker phosphorous layers, alongside a thin boundary film, on the flank surface of the tool. They attributed the formation of the phosphorous tribofilm to the heat generated at high drilling speeds, which promotes the chemical reaction with the metal surface. Also, in the same investigation, they applied another fluid, namely, polymer-based ester. As per their discussion, the tribofilm generated in the polymer-based ester primarily consists of carbon, accompanied by some traces of oxygen. This observation suggests a potential similarity in the case of CSF 35.

Another study, conducted by Luka et al. [46], validated the proposed percentage of friction coefficient reduction. They utilised an open tribotester to evaluate the frictional behaviour of identical workpiece and cutting tool materials as those used in this study. Their findings revealed a comparable reduction of up to 74% in the friction coefficient when employing a 5% emulsion, in contrast to dry conditions. Additionally, they confirmed a similar decreasing trend in friction coefficient values as sliding speeds increased, aligning closely with the range of COF values observed in this work.

3.4. Wettability Analysis

In Figure 9, the interaction between the droplet of each applied MWF and the workpiece material surface is depicted. Notably, CSF 35 oil displayed the highest contact angle, measuring up to 40^0, indicating its relatively lower wettability. Conversely, emulsions like Vasco 6000 and Zubora 67H exhibited easier droplet spreading, evidenced by reductions in the contact angle by 33% and 65%, respectively. This wettability behaviour of synthetic and semi-synthetic cutting fluids was confirmed in a previous work [47]. Hence, Zubora 67H was proven to be the optimal choice as a MWF in the secondary shear zone due to its exceptional wettability characteristics and its lowest viscosity index, leading to its superior performance in the secondary shear zones.

The improved wettability observed in synthetic and semi-synthetic emulsion cutting fluids is primarily attributed to the specific chemical composition inherent in the emulsion structure [48]. According to the supplier specifications and FTIR results, this composition typically consists of surfactants and various additives, such as carboxylic acid [49] and alkanolamides, which enhance the dispersion of oil in water [50]. This enhanced dispersion

significantly improves the spreadability of oil droplets across the metal surface by effectively reducing the surface tension of the oil droplets [51]. This reduction in surface tension promotes easier and more uniform coverage on the material being worked upon.

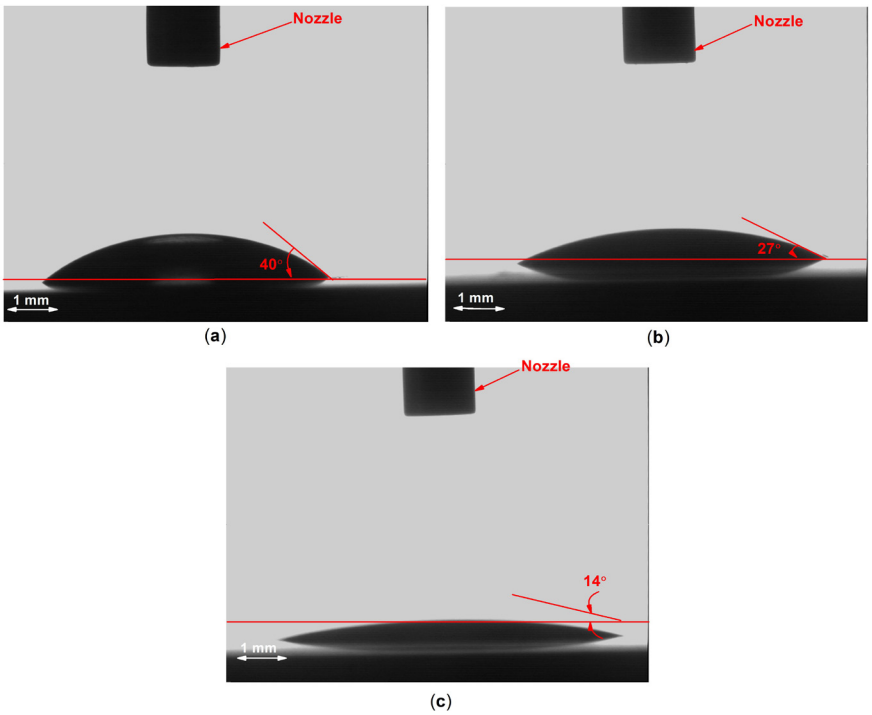

Figure 9. Wettability characteristics of (**a**) CSF 35, (**b**) Vasco 6000, and (**c**) Zubora 67H.

Moreover, the molecular structure within the emulsion exhibits a higher level of affinity towards the metal surface, owing to the presence of some compounds, such as phosphoric acid esters [52]. This chemical affinity allows the emulsion molecules to align and adhere more uniformly to the metal surface. As a result, this enhanced adhesion amplifies the overall wettability, facilitating improved interaction and coverage across the metal surface.

Regarding Zubora 67H type, it has higher amounts of polar additives, according to the manufacturer specifications. The presence of these polar additives, typically containing functional groups like hydroxyl (−OH), carbonyl (C=O), or other polar moieties, serves to strengthen the affinity of the lubricant to metal surfaces. The polar nature of these additives enables them to form stronger bonds or interactions with the metal surface. Conversely, the non-polar end of these molecules involves longer fatty acid chains orienting themselves away from the metal surface and towards the oil or lubricant [53]. This increased interaction leads to improved adhesion, ensuring a more effective and reliable coating of the lubricant on the metal surfaces.

3.5. Comparison with In Situ Measured Coefficient of Friction during Orthogonal Cutting

The planing test rig is used to measure the process force and to calculate the local normal stress σ and tangential stress τ at the cutting edge according to the method of Bergmann [29]. This method was used in [54] to determine the internal stresses of the cutting wedge during planing, as well in order to determine the mechanical load in wet metal cutting [55] and in combination with FE-based simulations to determine wear-optimised cutting edge microgeometries [56]. In the experiments, the cutting speed (V_c) is varied in three steps. The sliding speed of the chip (V_{chip}) on the rake face can be calculated according to Merchant, as shown in Equation (3) [57].

$$V_{chip} = (\sin \varphi / \cos(\varphi - \gamma)) V_c, \quad (3)$$

where φ is the shear angle, γ is the rake angle, and V_c is the cutting speed. The shear angle φ is measured via the high-speed recordings during the planing experiments.

In Figure 10, the normal and tangential stress in dependence of the cutting speed V_c during dry cutting is shown. Due to low forces and the associated high measurement uncertainty in the area of the detachment point of the chip on the rake face, areas for normal stresses σ below 0.5 GPa were not considered. Because of high plastic deformation at the cutting edge, coulomb-friction is not applicable [58]. Therefore, the local friction coefficient was calculated only on the rake face of the tool in the secondary shear zone. In this area, the local COF can be determined according to Equation (4).

$$\mu = \sigma/\tau, \tag{4}$$

where σ is the normal stress, τ is the tangential stress, and μ is the COF.

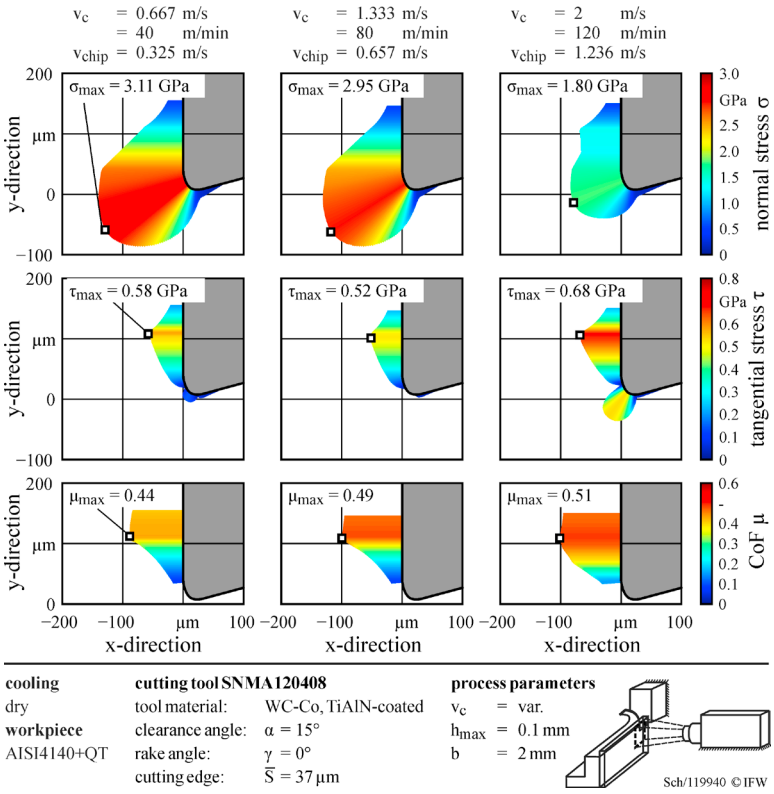

Figure 10. Normal stress, tangential stress, and local coefficient of friction during orthogonal cutting under variations of the cutting speed.

It can be seen that constant normal stresses were measured in the area of the cutting edge, whereas there was a regressive decrease in normal stress in the area of the secondary shear zone on the rake face of the tool. The maximum normal stresses occurred independently of the cutting speed in the area of the cutting edge rounding. At a cutting speed of V_c = 0.667 m/s, a maximum normal stress of 3.11 GPa was reached. As the cutting speed increased, the maximum normal stress decreased due to the thermal softening of the material as a result of higher relative speeds and, consequently, friction. The behaviour of the COF varied from the findings in the open tribotesting, except for its validation at 0.4 m/s. This was mainly due to the sliding speed change, which significantly reduced the normal pressure. However, in the open tribosystem, the hypothesis was established by keeping the pressure value constant at different sliding speeds, considering the constraint that the open tribotester can only achieve a maximum normal stress of 2 GPa.

With regard to the maximum tangential stress, there was an increase as the cutting speed increased. At the cutting edge, there was a point where the tangential stress was

equal to zero. At this point, there was no material flow, and therefore no Coulomb-COF was able to be calculated. In regions near to this point, there was a high amount of plastic deformation and separation occurring. As a result, the local coefficient of friction was only calculated on the rake face of the tool in the secondary shear zone where the plastic deformation of the chip was negligible.

Figure 11 illustrates the coefficient of friction (COF) trend behaviour at 0.5 and 1 GPa across a broad range of sliding speeds. In situ COF values, derived from the actual metal cutting process, exhibited a similar increasing pattern to those measured by the open tribometer. However, a notable difference of up to 33% in COF values was observed. This disparity is attributed to significant variances in the temperature and temperature gradient within the secondary shear zone compared to the open tribometer conditions. This finding aligns with assertions made in previous research articles [8,12,17], where authors highlighted challenges in replicating the same pressure and temperature gradient between rubbing contacts using tribotesters, particularly due to variations along the secondary shear zone.

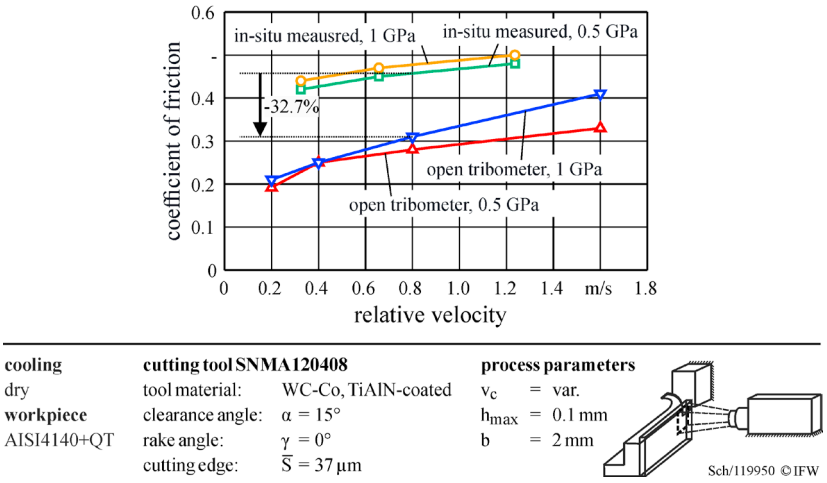

Figure 11. Comparison of friction coefficients determined in-situ during orthogonal cutting and using a tribometer as a function of relative velocity and normal stresses.

The study suggests that addressing the pressure effect is achievable by tailoring the pressure value using a high-pressure range tribotester (open tribotester) to mimic specific regions in the secondary shear zone. This approach enables the prediction of COF values while considering the associated error. However, controlling the temperature gradient necessitates variations through a heating system to simulate the actual cutting conditions, providing a potential path for future research to enhance experimental accuracy and reproducibility in this critical parameter.

4. Conclusions

In this comprehensive investigation, the frictional behaviour within the secondary shear zone was thoroughly explored using a customised ball-on-disc open tribometer. The key findings are summarised as follows:

- All applied cutting fluids experienced Newtonian attitude at up to 40 °C. At 60 °C, the emulsion-based oils started showing shear thinning behaviour, and this phenomenon significantly increased, especially for Zubora 67H, as the temperature increased further.
- CSF 35 displayed the lowest dynamic viscosity, attributed to the absence of certain polar additives found in emulsions. However, it can sustain viscosity at higher temperatures, thanks to its highest viscosity index.
- The COF obtained from tribometer testing in dry conditions showcased a noteworthy increase at contact pressures of up to 1 GPa. However, at 2 GPa, the COF trend exhibited a marked decrease. This reversal could potentially be ascribed to three factors:

increased heat dissipation at higher speeds, a reduced impact of surface irregularities on the friction coefficient, and thermal softening resulting from increased pressure.

- COF values under lubricated conditions highlighted the capability of emulsion-based oils, particularly Zubora 67H, to achieve a reduction of up to 78%. This reduction was attributed to the influence of polar additives enhancing frictional behaviour.
- The physical characteristics of the applied MWFs were evaluated by measuring the contact angle with the steel surface. Emulsions, especially Zubora 67H, demonstrated a significant improvement in wettability characteristics, evidenced by a 65% reduction in the contact angle compared to CSF 35.
- The local coefficient of friction in the secondary shear zone of the rake face can be calculated due to high-speed recordings and measurements of the process forces.
- The in situ-measured COFs in cutting showed the same trend as the measured COFs on the open tribometer regarding an increase in the relative velocity. However, there was a difference in the absolute values due to the high temperature and high temperature gradients in the cutting processes which were not present at the open tribometer.

A key recommendation for future investigations involves addressing temperature fluctuations within the rubbing contact. This strategic focus aims to enhance the precision of simulating real cutting conditions using the constructed open tribotester, with an anticipated consequential reduction in the calculated error. This emphasis on temperature control highlights a commitment to refining experimental methodologies for more robust and accurate outcomes in subsequent research endeavours.

Author Contributions: Conceptualisation, B.G.N., F.P., G.P., J.S., B.B. and B.D.; methodology, B.G.N., F.P., J.S. and B.B.; samples preparation, B.G.N. and J.S.; validation, B.G.N., F.P., J.S. and B.B.; formal analysis, B.G.N. and J.S.; investigation, B.G.N. and J.S.; resources, F.P. and B.B.; data curation, B.G.N., F.P., B.B. and J.S.; writing—original draft preparation, B.G.N. and J.S.; writing—review and editing, G.P., F.P., B.D. and B.B.; visualisation, G.P., F.P., B.G.N., B.D., B.B. and J.S.; project administration, G.P., B.D., F.P. and B.B. All authors have read and agreed to the published version of the manuscript.

Funding: The authors appreciate the funding of this work within the Priority Program 2231 "Efficient cooling, lubrication and transportation—coupled mechanical and fluid-dynamical simulation methods for efficient production processes (FLUSIMPRO)" by the German Research Foundation (DFG)—project number 439904924. The publication of this article was funded by the Open Access Fund of Leibniz Universität Hannover.

Data Availability Statement: Data are contained within the article.

Acknowledgments: We express our sincere appreciation to Netszch GmbH in Germany for their invaluable assistance with the rotational rheometer. Additionally, heartfelt thanks are extended to the Institute for Multiphase Processes (IMP) at Leibniz University Hannover, Germany, for their valuable support in conducting wettability tests.

Conflicts of Interest: The authors declare no conflicts of interest.

References

1. Shashidhara, Y.; Jayaram, S. Vegetable oils as a potential cutting fluid—An evolution. *Tribol. Int.* **2010**, *43*, 1073–1081. [CrossRef]
2. Khan, M.A.A.; Hussain, M.; Lodhi, S.K.; Zazoum, B.; Asad, M.; Afzal, A. Green Metalworking Fluids for Sustainable Machining Operations and Other Sustainable Systems: A Review. *Metals* **2022**, *12*, 1466. [CrossRef]
3. Vardhanapu, M.; Chaganti, P.K. A review on testing methods of metalworking fluids for environmental health. *Mater. Today Proc.* **2020**, *26*, 2405–2411. [CrossRef]
4. Ogedengbe, T.S.; Awe, P.; Joseph, O.I. Comparative analysis of machining stainless steel using soluble and vegetable oils as cutting fluids. *Int. J. Manu. Mater. Mech. Eng.* **2019**, *4*, 33–40. [CrossRef]
5. Sharma, A.K.; Tiwari, A.K.; Dixit, A.R. Effects of Minimum Quantity Lubrication (MQL) in machining processes using conventional and nanofluid based cutting fluids: A comprehensive review. *J. Clean. Prod.* **2016**, *127*, 1–18. [CrossRef]
6. Irani, R.; Bauer, R.; Warkentin, A. A review of cutting fluid application in the grinding process. *Int. J. Mach. Tools Manuf.* **2005**, *45*, 1696–1705. [CrossRef]
7. de Eguilaz, E.R.; Rech, J.; Arrazola, P. Characterization of friction coefficient and heat partition coefficient between an AISI4140 steel and a TiN-coated carbide—Influence of (Ca, Mn, S) steel's inclusions. *Proc. Inst. Mech. Eng. Part J J. Eng. Tribol.* **2010**, *224*, 1115–1127. [CrossRef]

8. Zemzemi, F.; Bensalem, W.; Rech, J.; Dogui, A.; Kapsa, P. New tribometer designed for the characterisation of the friction properties at the tool/chip/workpiece interfaces in machining. *Lubr. Sci.* **2008**, *14*, 11–25. [CrossRef]
9. Özel, T. The influence of friction models on finite element simulations of machining. *Int. J. Mach. Tools Manuf.* **2006**, *46*, 518–530. [CrossRef]
10. Trent, E.M.; Wright, P.K. Metal cutting, (4th edition), "Butterworth-Heinemann", Boston, 2000. *Sci. Sinter.* **2004**, *36*, 446. [CrossRef]
11. Melkote, S.N.; Grzesik, W.; Outeiro, J.; Rech, J.; Schulze, V.; Attia, H.; Arrazola, P.-J.; M'Saoubi, R.; Saldana, C. Advances in material and friction data for modelling of metal machining. *CIRP Ann. Manuf. Technol.* **2017**, *66*, 731–754. [CrossRef]
12. Grzesik, W.; Rech, J. Development of tribo-testers for predicting metal cutting friction. *J. Mach. Eng.* **2019**, *19*, 62–70. [CrossRef]
13. Wiklund, U.; Wänstrand, O.; Larsson, M.; Hogmark, S. Evaluation of new multilayered physical vapour deposition coatings in sliding contact. *Wear* **1999**, *236*, 88–95. [CrossRef]
14. Hogmark, S.; Hedenqvist, P.; Jacobson, S. Tribological properties of thin hard coatings: Demands and evaluation. *Surf. Coat. Technol.* **1997**, *90*, 247–257. [CrossRef]
15. Pape, F.; Poll, G.; Ellersiek, L.; Denkena, B.; Liu, H. Tribological Effects of Metalworking Fluids in Cutting Processes. *Lubricants* **2023**, *11*, 224. [CrossRef]
16. Liu, H.C.; Pape, F.; Zhao, Y.; Ellersiek, L.; Denkena, B.; Poll, G. On the Elastohydrodynamic Film-Forming Properties of Metalworking Fluids and Oil-in-Water Emulsions. *Tribol. Lett.* **2022**, *71*, 10. [CrossRef]
17. Grzesik, W.; Zalisz, Z.; Nieslony, P. Friction and wear testing of multilayer coatings on carbide substrates for dry machining applications. *Surf. Coat. Technol.* **2002**, *155*, 37–45. [CrossRef]
18. Hedenqvist, P.; Olsson, M. Sliding wear testing of coated cutting tool materials. *Tribol. Int.* **1991**, *24*, 143–150. [CrossRef]
19. Claudin, C.; Mondelin, A.; Rech, J.; Fromentin, G. Effects of a straight oil on friction at the tool–workmaterial interface in machining. *Int. J. Mach. Tools Manuf.* **2010**, *50*, 681–688. [CrossRef]
20. Bonnet, C.; Valiorgue, F.; Rech, J.; Claudin, C.; Hamdi, H.; Bergheau, J.; Gilles, P. Identification of a friction model—Application to the context of dry cutting of an AISI 316L austenitic stainless steel with a TiN coated carbide tool. *Int. J. Mach. Tools Manuf.* **2008**, *48*, 1211–1223. [CrossRef]
21. Rech, J.; Arrazola, P.J.; Claudin, C.; Courbon, C.; Pusavec, F.; Kopac, J. Characterisation of friction and heat partition coefficients at the tool-work material interface in cutting. *CIRP Ann. Manuf. Technol.* **2013**, *62*, 79–82. [CrossRef]
22. Priest, J.; Ghadbeigi, H.; Ayvar-Soberanis, S.; Liljerehn, A.; Way, M. Analysis of the contact mechanics in machining using a novel high-speed tribometer. *Procedia CIRP* **2022**, *108*, 123–128. [CrossRef]
23. Sadowski, P.; Stupkiewicz, S. Friction in lubricated soft-on-hard, hard-on-soft and soft-on-soft sliding contacts. *Tribol. Int.* **2019**, *129*, 246–256. [CrossRef]
24. Randall, N.X. Experimental Methods in Tribology. In *Tribology for Scientists and Engineers: From Basics to Advanced Concepts*; Menezes, P.L., Nosonovsky, M., Ingole, S.P., Kailas, S.V., Lovell, M.R., Eds.; Springer: New York, NY, USA, 2013; pp. 141–175. [CrossRef]
25. Wang, L.; Cai, J.; Zhou, J.; Duszczyk, J. Characteristics of the Friction Between Aluminium and Steel at Elevated Temperatures During Ball-on-Disc Tests. *Tribol. Lett.* **2009**, *36*, 183–190. [CrossRef]
26. Peng, B.; Spikes, H.; Kadiric, A. The Development and Application of a Scuffing Test Based on Contra-rotation. *Tribol. Lett.* **2019**, *67*, 37. [CrossRef]
27. Ingram, M.; Hamer, C.; Spikes, H. A new scuffing test using contra-rotation. *Wear* **2015**, *328–329*, 229–240. [CrossRef]
28. Lakner, T.; Hardt, M. A Novel Experimental Test Bench to Investigate the Effects of Cutting Fluids on the Frictional Conditions in Metal Cutting. *J. Manuf. Mater. Process.* **2020**, *4*, 45. [CrossRef]
29. Bergmann, B. Grundlagen zur Auslegung von Schneidkantenverrundungen; TEWISS. Ph.D. Thesis, Leibniz University, Hanover, Germany, 2018.
30. Bair, S.; Vergne, P.; Kumar, P.; Poll, G.; Krupka, I.; Hartl, M.; Habchi, W.; Larsson, R. Comment on "History, origins and prediction of elastohydrodynamic friction" by Spikes and Jie. *Tribol. Lett.* **2015**, *58*, 16. [CrossRef]
31. Yan, Y.D.; Dhont, J.K.G.; Smits, C.; Lekkerkerker, H.N.W. Oscillatory-shear-induced order in nonaqueous dispersions of charged colloidal spheres. *Phys. A Stat. Mech. Appl.* **1994**, *202*, 68–80. [CrossRef]
32. Nassef, B.G.; Pape, F.; Poll, G. Enhancing the Performance of Rapeseed Oil Lubricant for Machinery Component Applications through Hybrid Blends of Nanoadditives. *Lubricants* **2023**, *11*, 479. [CrossRef]
33. López-Barrón, C.R.; Wagner, N.J.; Porcar, L. Layering, melting, and recrystallization of a close-packed micellar crystal under steady and large-amplitude oscillatory shear flows. *J. Rheol.* **2015**, *59*, 793–820. [CrossRef]
34. Fagundes, F.M.; Santos, N.B.; Damasceno, J.J.R.; Arouca, F.O. Study on the stability of a shear-thinning suspension used in oil well drilling. *Oil Gas Sci. Technol.* **2018**, *73*, 10. [CrossRef]
35. Sjöblom, J.; Stenius, P.; Simon, S.; Grimes, B.A. Emulsion Stabilization. In *Encyclopedia of Colloid and Interface Science*; Tadros, T., Ed.; Springer: Berlin/Heidelberg, Germany, 2013; pp. 415–454. [CrossRef]
36. Yaghi, B.M.; Al-Bemani, A. Heavy Crude Oil Viscosity Reduction for Pipeline Transportation. *Energy Sources* **2002**, *24*, 93–102. [CrossRef]
37. Souas, F.; Safri, A.; Benmounah, A. A review on the rheology of heavy crude oil for pipeline transportation. *Pet. Res.* **2021**, *6*, 116–136. [CrossRef]

38. Jamaluddin, N.A.; Talib, N.; Sani, A.S.A. Tribological assessment of modified Jatropha oil with hBN and graphene nanoparticles as a new preference for the metalworking fluid. *Int. J. Eng. Adv. Technol.* **2020**, *9*, 3144–3149. [CrossRef]
39. Yang, K.Z.; Pramanik, A.; Basak, A.K.; Dong, Y.; Prakash, C.; Shankar, S.; Dixit, S.; Kumar, K.; Ivanovich Vatin, N. Application of coolants during tool-based machining—A review. *Ain Shams Eng. J.* **2023**, *14*, 101830. [CrossRef]
40. Rech, J. A multiview approach to the tribological characterisation of cutting tool coatings for steels in high-speed dry turning. *Int. J. Mach. Mach. Mater.* **2006**, *1*, 27–44. [CrossRef]
41. Oshio, T. Anti-Wear Properties and Mechanisms of Dialkyl Phosphonates in Ester Base Oils. Ph.D. Thesis, Ecole Centrale de Lyon, Écully, France, 2023. (In English).
42. Beltzer, M.; Jahanmir, S. Effect of additive molecular structure on friction. *Lubr. Sci.* **1988**, *1*, 3–26. [CrossRef]
43. Minami, I.; Mori, S. Concept of molecular design towards additive technology for advanced lubricants. *Lubr. Sci.* **2007**, *19*, 127–149. [CrossRef]
44. Tang, Z.; Li, S. A review of recent developments of friction modifiers for liquid lubricants (2007–present). *Curr. Opin. Solid State Mater. Sci.* **2014**, *18*, 119–139. [CrossRef]
45. Ma, J.; Mohammadi, J.; Zhou, Y.; Larsh, J.; Januszkiewicz, K.; Evans, R.; Zhao, Y.; Gali, O.A.; Riahi, R.A. An investigation into cutting fluid additives performance during machining processing of Ti-6Al-4V. *Int. J. Adv. Manuf. Technol.* **2021**, *112*, 977–987. [CrossRef]
46. Sterle, L.; Pušavec, F.; Kalin, M. Determination of friction coefficient in cutting processes: Comparison between open and closed tribometers. *Procedia CIRP* **2019**, *82*, 101–106. [CrossRef]
47. Iowa Waste Reduction Center. *Cutting Fluid Management: Small Machining Operations*; Iowa Waste Reduction Center: Cedar Falls, IA, USA, 2003.
48. Bienkowski, K. *Coolants and Lubricants: The Truth*; Manufacturing Engineering: Oakland, CA, USA, 1993; pp. 90–92.
49. Wang, S.-H.; Yue, J.; Dong, W.; Zuo, T.-T.; Li, J.-Y.; Liu, X.; Zhang, X.-D.; Liu, L.; Shi, J.-L.; Yin, Y.-X. Tuning wettability of molten lithium via a chemical strategy for lithium metal anodes. *Nat. Commun.* **2019**, *10*, 4930. [CrossRef] [PubMed]
50. Pu, D.; Xiong, Y.-c.; Feng, R.-s.; Guo, Y.-j.; Lin, L.; Xu, C.-j.; Yu, W.-k. Study on the Adaptability of Alkanolamide (LDEA) Lowering Oil/Water Interfacial Tension to Different Crude Oils. *J. Surfactants Deterg.* **2020**, *23*, 1145–1157. [CrossRef]
51. Li, Y.; Duan, Y.-Z.; Zhang, K. Effect of Alkanolamide on Interfacial Tension and Loss of Petroleum Sulfonates for Enhanced Oil Recovery. *J. Dispers. Sci. Technol.* **2010**, *31*, 722–726. [CrossRef]
52. Aguilar-Mendoza, J.A.; Rosales-Leal, J.I.; Rodríguez-Valverde, M.A.; Cabrerizo-Vílchez, M.A. Effect of acid etching on dentin wettability and roughness: Self-etching primers versus phosphoric acid. *J. Biomed. Mater. Res. Part B Appl. Biomater.* **2008**, *84B*, 277–285. [CrossRef] [PubMed]
53. Wakabayashi, T. Cutting Fluid. In *CIRP Encyclopedia of Production Engineering*; Laperrière, L., Reinhart, G., Eds.; Springer: Berlin, Germany, 2014; pp. 311–315. [CrossRef]
54. Denkena, B.; Bergmann, B.; Picker, T.; Kraeft, M. Modeling of stresses at the cutting wedge in the interrupted cut for the design of the cutting edge microgeometry. *Procedia CIRP* **2023**, *117*, 299–304. [CrossRef]
55. Denkena, B.; Liu, H.C.; Pape, F.; Bergmann, B.; Poll, G.; Schenzel, J.; Ellersiek, L. Simulation of local contact conditions in the secondary shear zone in dry and wet metal cutting. *Procedia CIRP* **2023**, *117*, 293–298. [CrossRef]
56. Bergmann, B.; Denkena, B.; Beblein, S.; Picker, T. FE-Simulation Based Design of Wear-Optimized Cutting Edge Roundings. *J. Manuf. Mater. Process.* **2021**, *5*, 126. [CrossRef]
57. Merchant, M.E. Mechanics of the Metal Cutting Process. I. Orthogonal Cutting and a Type 2 Chip. *J. Appl. Phys.* **2004**, *16*, 267–275. [CrossRef]
58. Zorev, N. Inter-relationship between shear processes occurring along tool face and shear plane in metal cutting. *Proc. Int. Prod. Eng. Res.* **1963**, *49*, 143–152.